

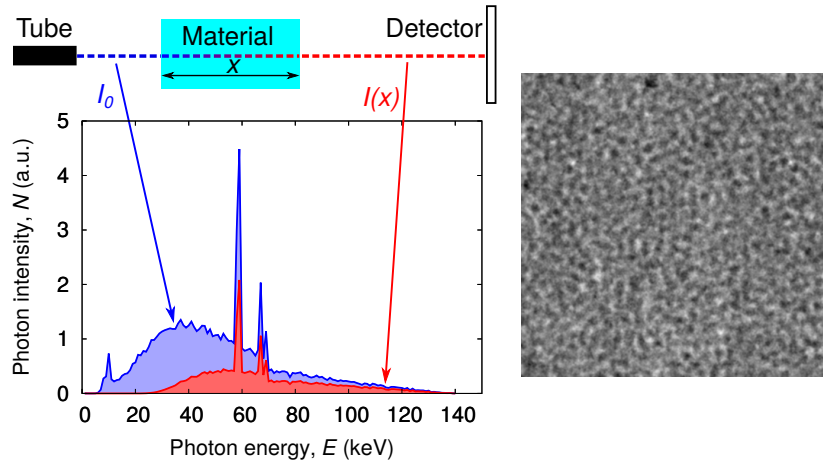


PhD defense
Manuel Baur

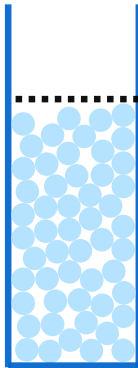
Funded by the German
Federal Ministry for
Economic Affairs and
Energy, grant no. 50WM

1653

X-ray radiography of granular systems – particle densities and dynamics

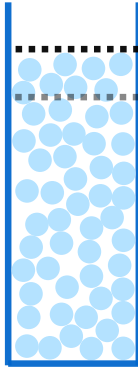


X-ray radiography of granular systems – particle densities and dynamics



$$\Phi = \text{RLP}$$

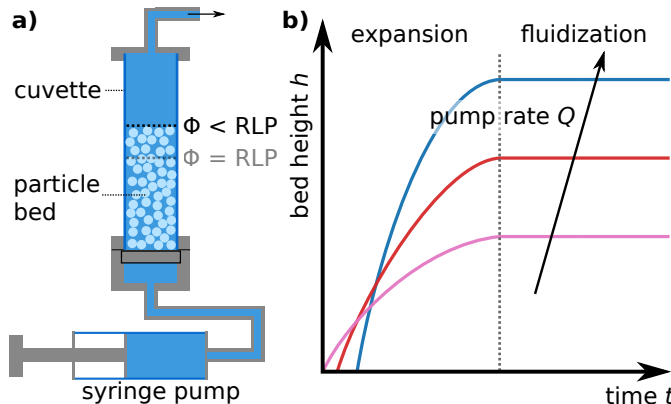
X-ray radiography of granular systems – particle densities and dynamics



$\Phi < \text{RLP}$
 $\Phi = \text{RLP}$

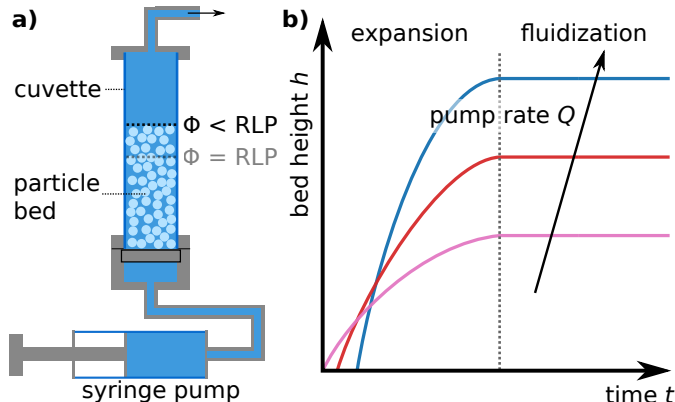
X-ray radiography of granular systems – particle densities and dynamics

Fluidized bed



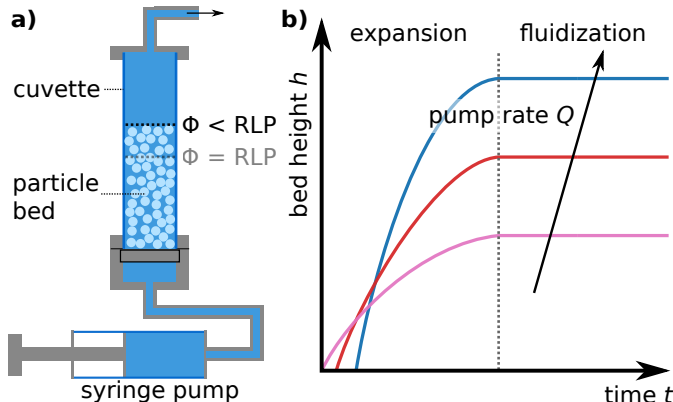
X-ray radiography of granular systems – particle densities and dynamics

Fluidized bed



X-ray radiography of granular systems – particle densities and dynamics

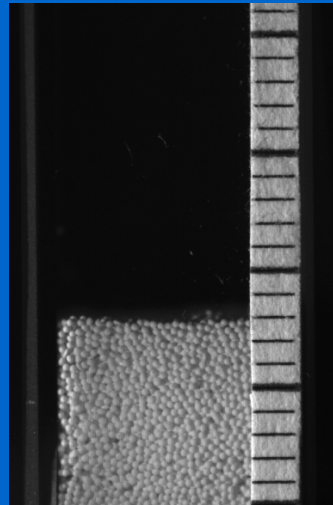
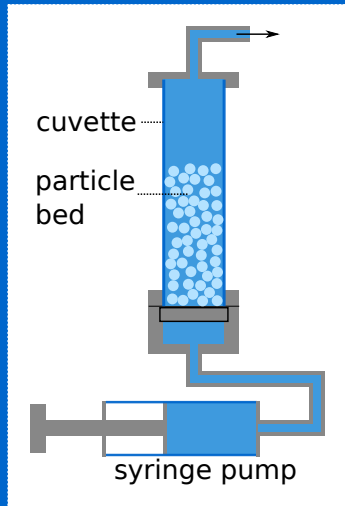
Fluidized bed



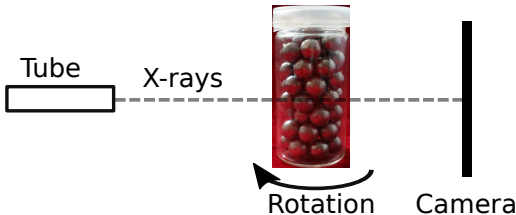
Fluidized bed reactor

"Lack of understanding:
It is very difficult to predict and calculate the **complex mass** [...] **flows** within the bed."

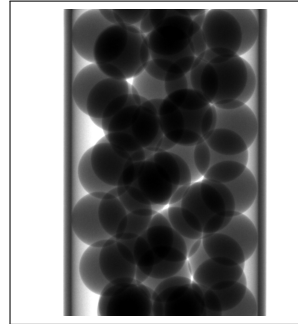
Particulate flows are **opaque**



X-ray radiography

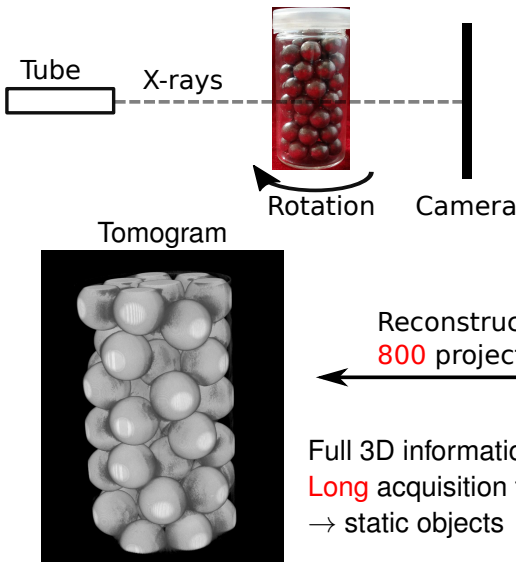


Radiogram



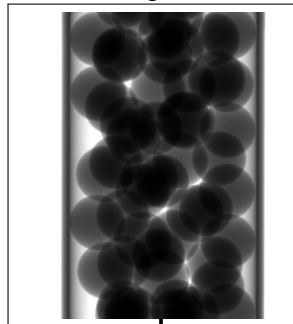
2D projections of 3D object
Short acquisition time

X-ray radiography

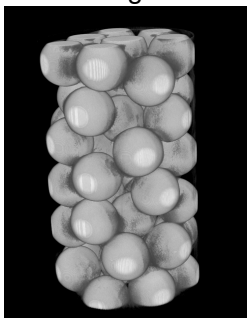


Radiogram

2D projections of 3D object
Short acquisition time

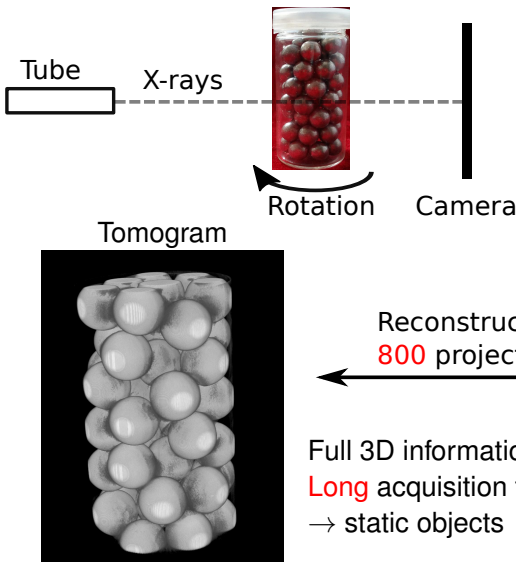


Reconstruction from
800 projections

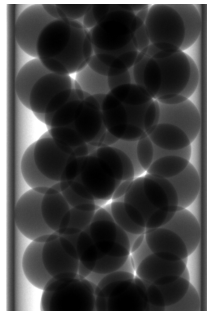


Full 3D information
Long acquisition time
→ static objects

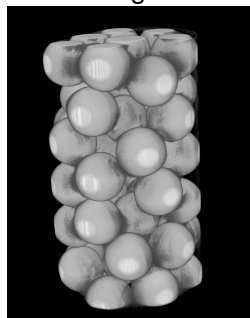
X-ray radiography



Radiogram

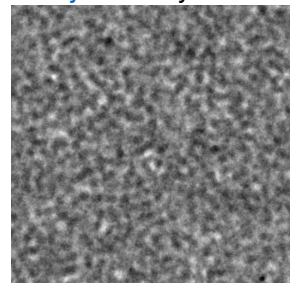


2D projections of 3D object
Short acquisition time

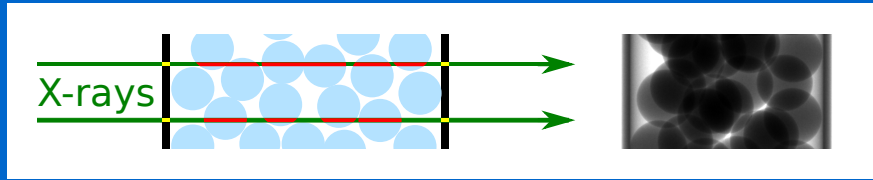


Full 3D information
Long acquisition time
→ static objects

Dynamic system



Measuring the volume fraction of **dynamic** granular systems

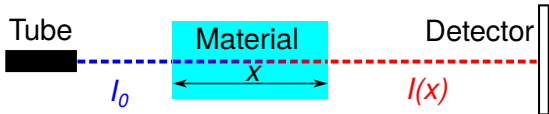


Correction of beam hardening
in X-ray radiograms

Baur *et al*, *Rev. Sci. Instrum.* (2019)

In collaboration with Norman Uhlmann, Fraunhofer EZRT

Attenuation of X-rays

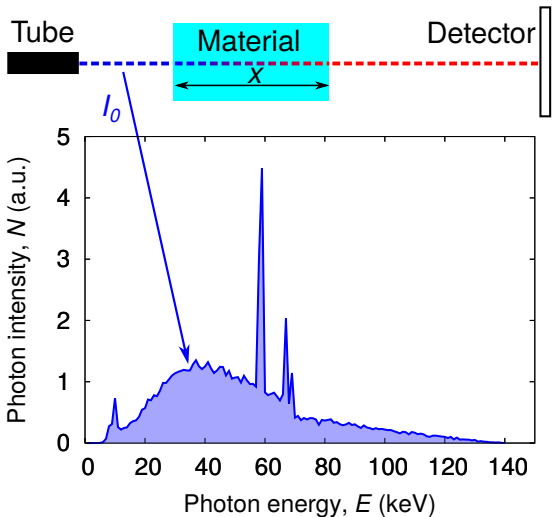


Beer-Lambert's law

$$I(x) = I_0 \exp(-\mu x)$$

$$\text{Thickness: } x = -\frac{1}{\mu} \ln \frac{I(x)}{I_0}$$

Attenuation of X-rays

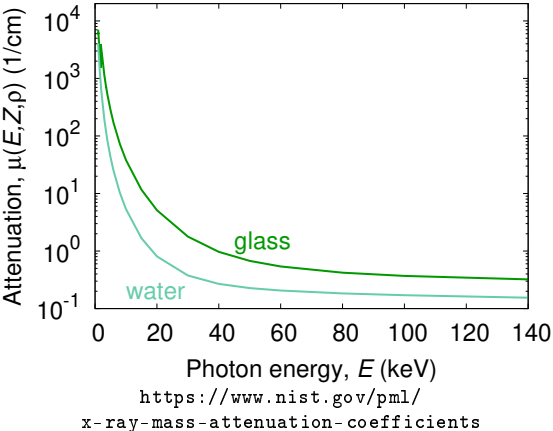


Beer-Lambert's law

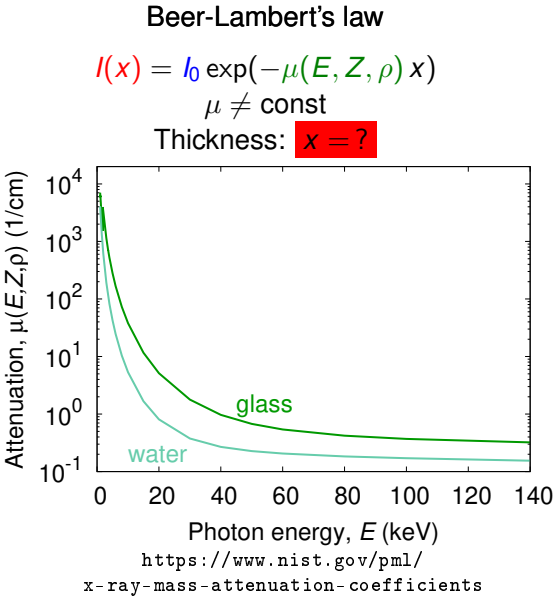
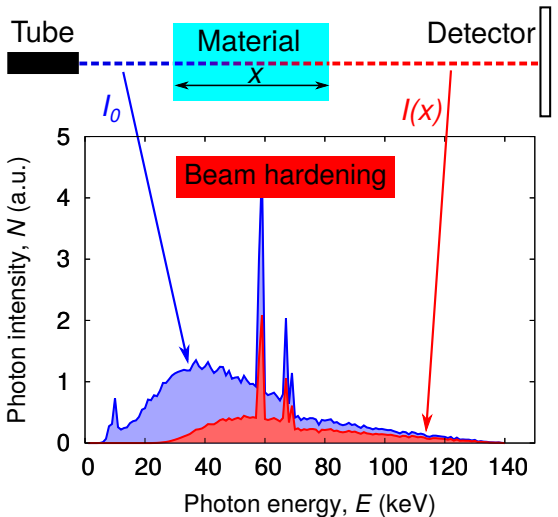
$$I(x) = I_0 \exp(-\mu(E, Z, \rho)x)$$

$\mu \neq \text{const}$

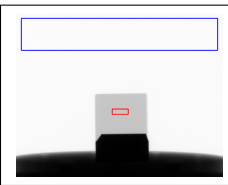
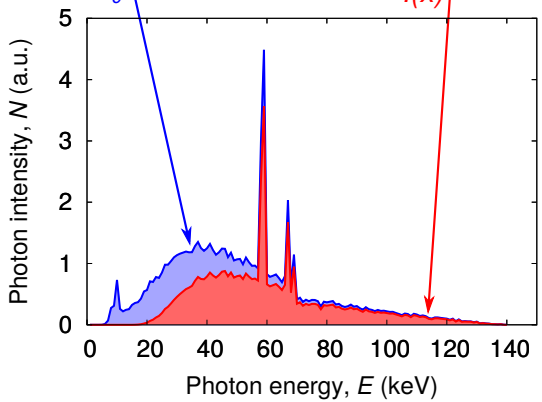
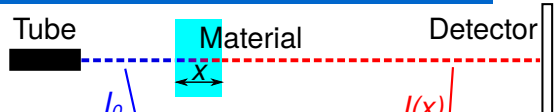
Thickness: $x = ?$



Attenuation of X-rays

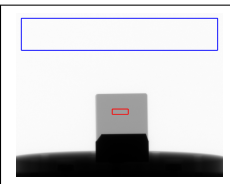
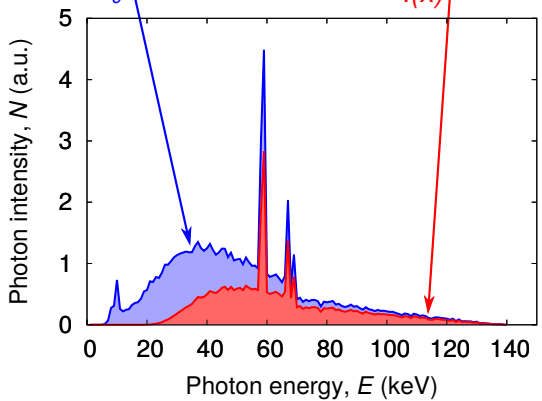
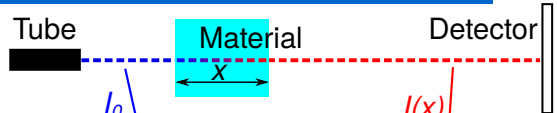


The effective attenuation, μ_{eff}



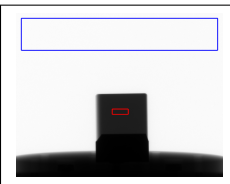
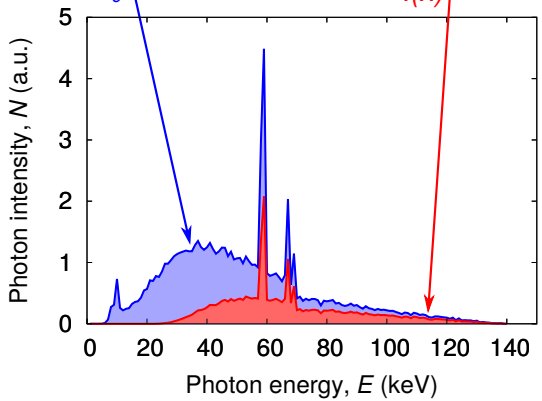
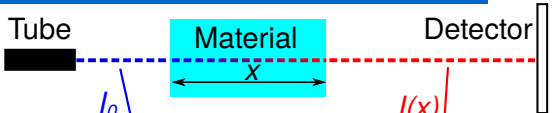
effective attenuation:
 $I(x) = I_0 \exp(-\mu_{\text{eff}}(x) x)$

The effective attenuation, μ_{eff}



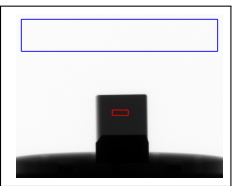
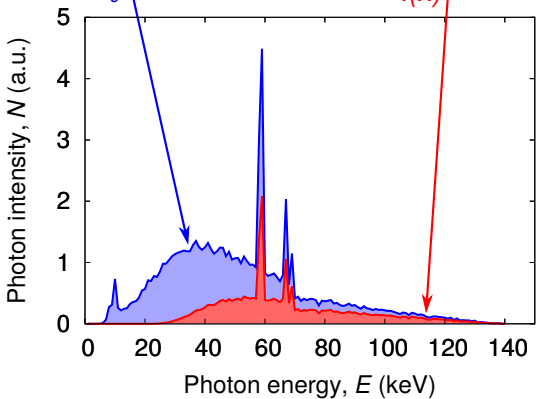
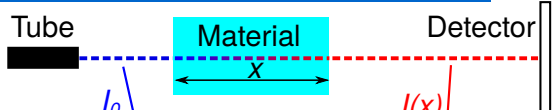
effective attenuation:
 $I(x) = I_0 \exp(-\mu_{\text{eff}}(x) x)$

The effective attenuation, μ_{eff}



effective attenuation:
 $I(x) = I_0 \exp(-\mu_{\text{eff}}(x) x)$

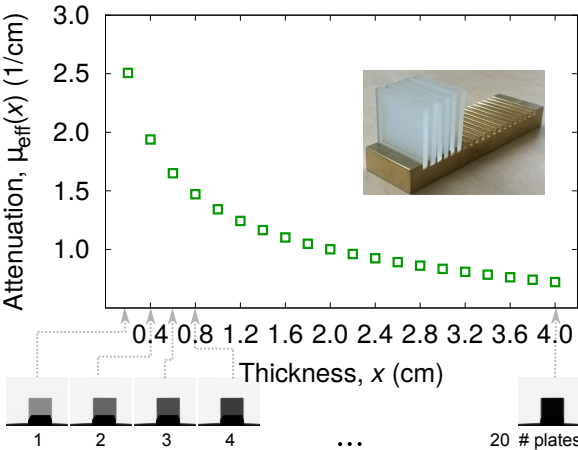
The effective attenuation, μ_{eff}



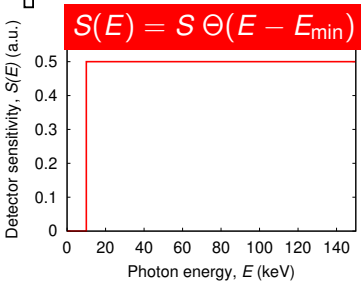
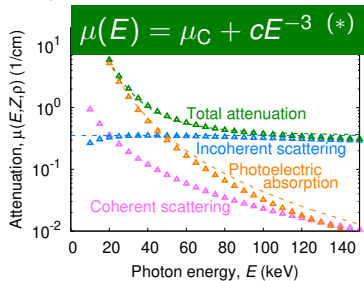
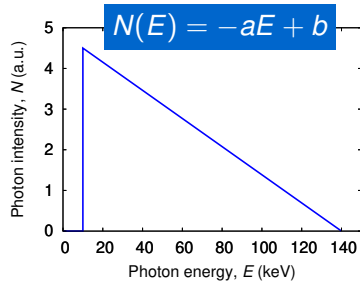
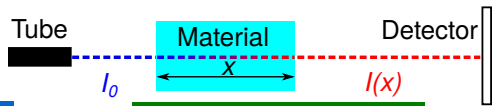
effective attenuation:

$$I(x) = I_0 \exp(-\mu_{\text{eff}}(x)x)$$

$$\mu_{\text{eff}}(x) = -\frac{1}{x} \frac{I(x)}{I_0}$$



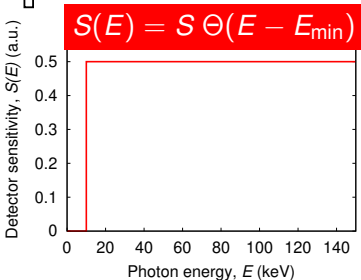
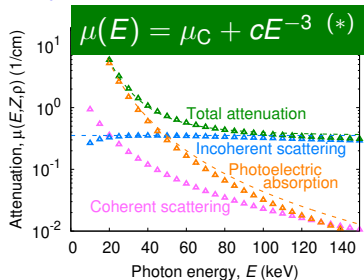
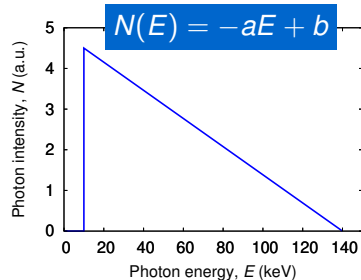
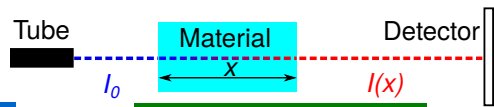
Modeling of μ_{eff}



$$I(x) \propto \int N(E) \exp\{-\mu(E, Z, \rho)x\} S(E) dE$$

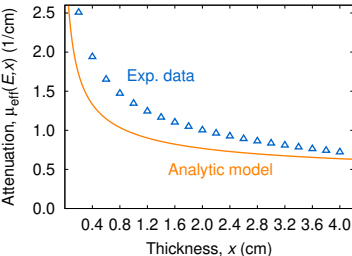
(*) XCOM supplied by NIST

Modeling of μ_{eff}



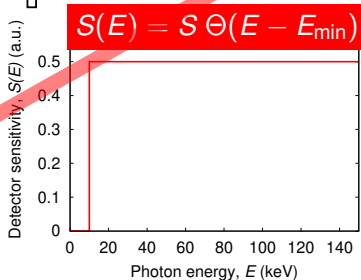
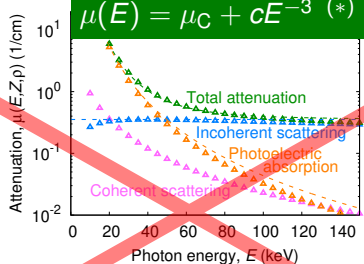
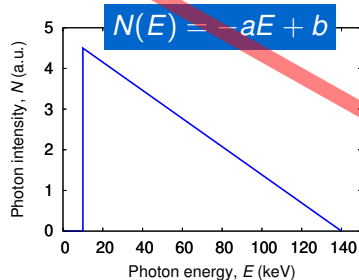
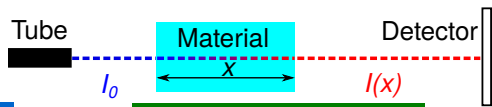
$$I(x) \propto \int N(E) \exp\{-\mu(E, Z, \rho)x\} S(E) dE$$

$$\propto S \int_{E_{\min}}^{E_{\max}} (-aE + b) \exp\{-(\mu_C + cE^{-3})x\} dE$$



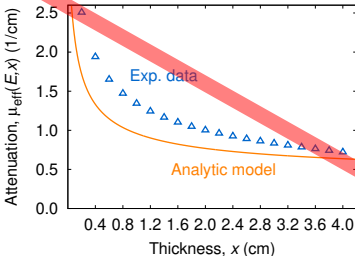
(*) XCOM supplied by NIST

Modeling of μ_{eff}

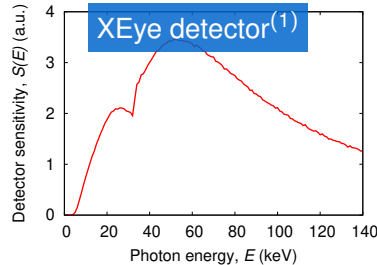
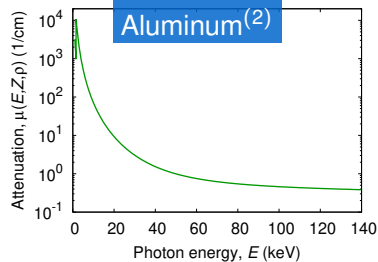
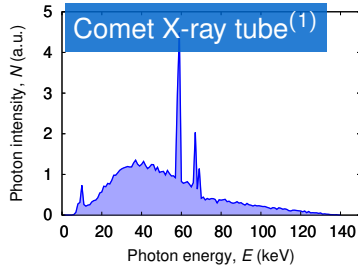
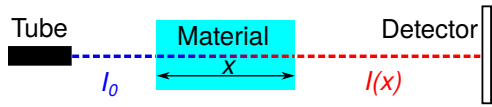


$$\begin{aligned} I(x) &\propto \int N(E) \exp\{-\mu(E, Z, \rho)x\} S(E) dE \\ &\propto S \int_{E_{\min}}^{E_{\max}} (-aE + b) \exp\{-(\mu_C + cE^{-3})x\} dE \end{aligned}$$

(*) XCOM supplied by NIST



Numerical approx. of μ_{eff}

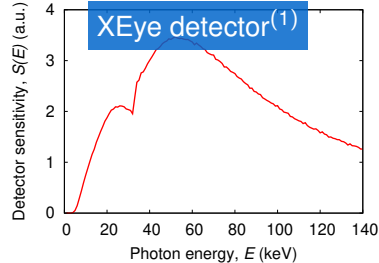
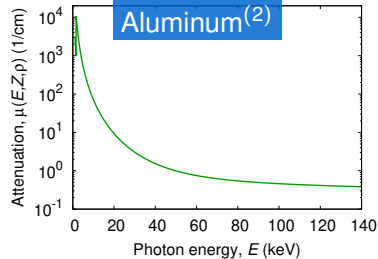
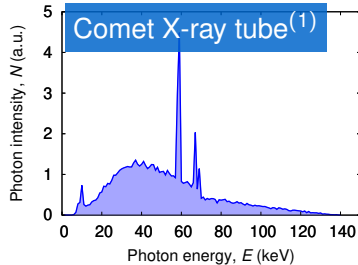
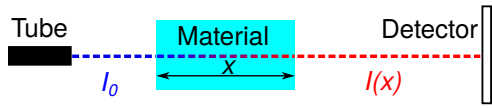


$$I(x) \propto \int N(E) \exp\{-\mu(E, Z, \rho)x\} S(E) dE$$
$$\int \rightarrow \sum$$

(1) Supplied by Norman Uhlmann, Fraunhofer EZRT

(2) XCOM supplied by NIST

Numerical approx. of μ_{eff}

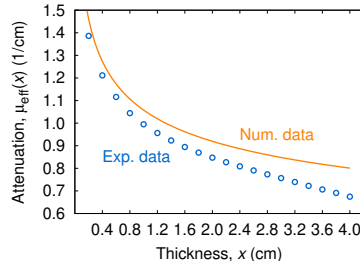


$$I(x) \propto \int N(E) \exp\{-\mu(E, Z, \rho)x\} S(E) dE$$

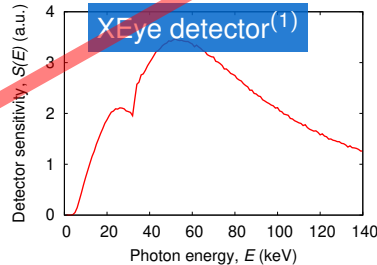
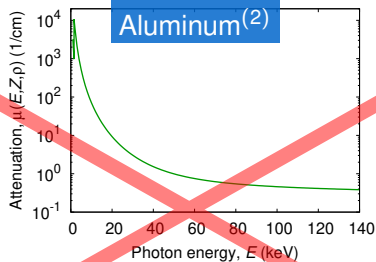
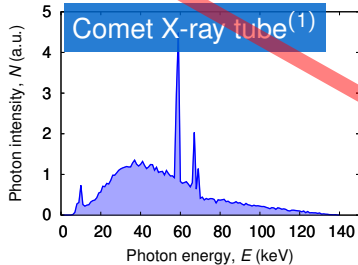
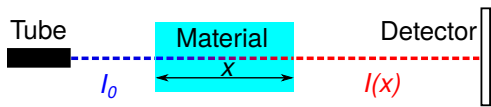
$$\int \rightarrow \sum$$

(1) Supplied by Norman Uhlmann, Fraunhofer EZRT

(2) XCOM supplied by NIST

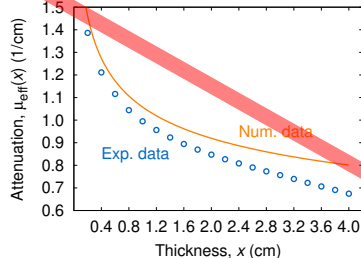


Numerical approx. of μ_{eff}



$$I(x) \propto \int N(E) \exp\{-\mu(E, Z, \rho)x\} S(E) dE$$

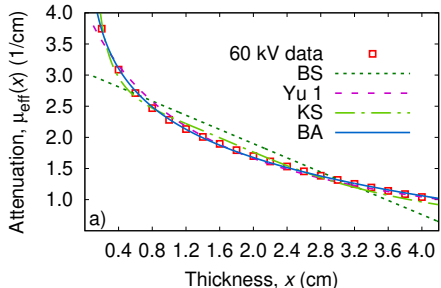
$$\int \rightarrow \sum$$



(1) Supplied by Norman Uhlmann, Fraunhofer EZRT

(2) XCOM supplied by NIST

Heuristic model functions for μ_{eff}



$$\mu_{\text{eff}}(x) = \mu_0 - \lambda x$$

Bjärngard & Shackford
(1994)

$$\mu_{\text{eff}}(x) = \frac{\mu_0}{1 + \lambda x}$$

Yu *et al.* (1997)

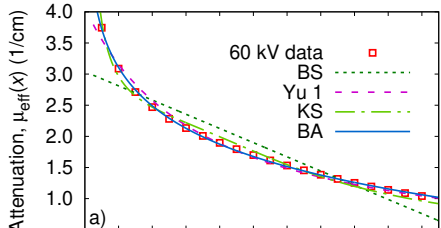
$$\mu_{\text{eff}}(x) = \mu(E_{\text{max}}) + \frac{2\mu_1}{x\sqrt{-\lambda_1^2+4\lambda_2}} \times \left[\arctan\left(\frac{\lambda_1+2\lambda_2x}{\sqrt{-\lambda_1^2+4\lambda_2}}\right) - \arctan\left(\frac{\lambda_1}{\sqrt{-\lambda_1^2+4\lambda_2}}\right) \right]$$

Kleinschmidt (1999)

$$\mu_{\text{eff}}(x) = a + \frac{b}{x^\alpha}$$

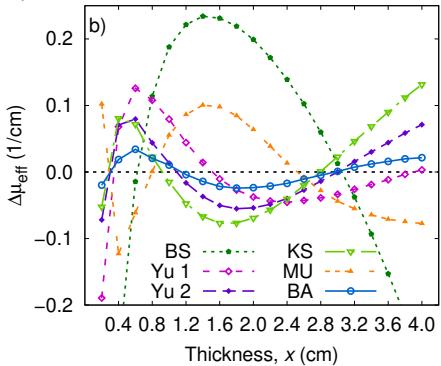
Baur *et al.* (2019)
(this work)

Heuristic model functions for μ_{eff}



$$\mu_{\text{eff}}(x) = \mu_0 - \lambda x$$

Bjärngard & Shackford
(1994)



$$\mu_{\text{eff}}(x) = \frac{\mu_0}{1+\lambda x}$$

$$\mu_{\text{eff}}(x) = \frac{\mu_0}{(1+\lambda x)^\beta}$$

Yu *et al.* (1997)

$$\mu_{\text{eff}}(x) = \mu(E_{\text{max}}) + \frac{2\mu_1}{x\sqrt{-\lambda_1^2+4\lambda_2}} \times \left[\arctan\left(\frac{\lambda_1+2\lambda_2 x}{\sqrt{-\lambda_1^2+4\lambda_2}}\right) - \arctan\left(\frac{\lambda_1}{\sqrt{-\lambda_1^2+4\lambda_2}}\right) \right]$$

Kleinschmidt (1999)

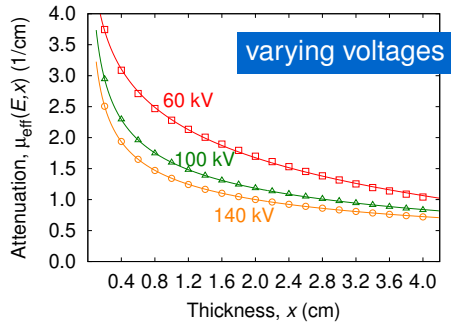
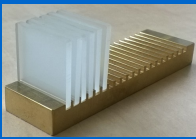
$$\mu_{\text{eff}}(x) = -\frac{1}{x} \ln [A + B \exp(-x/C)]$$

Mudde *et al.* (2008)

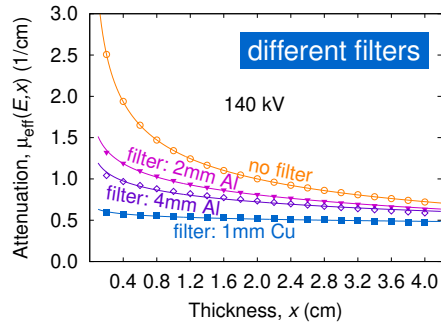
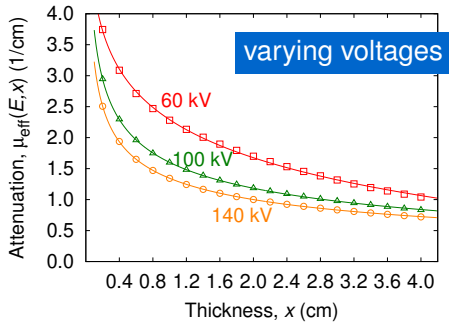
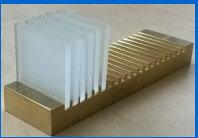
$$\mu_{\text{eff}}(x) = a + \frac{b}{x^\alpha}$$

Baur *et al.* (2019)
(this work)

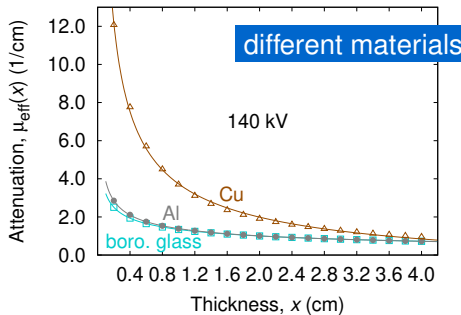
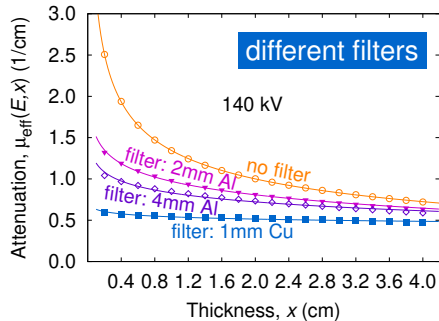
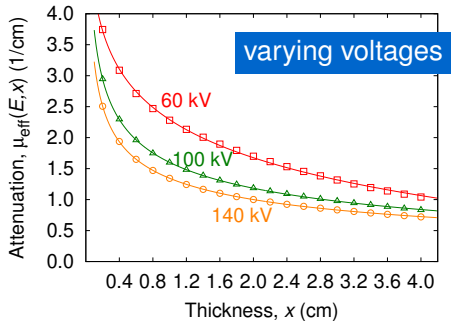
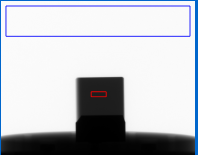
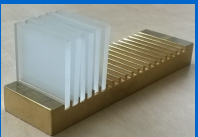
Universality of
 $\mu_{\text{eff}}(x) = a + \frac{b}{x^\alpha}$



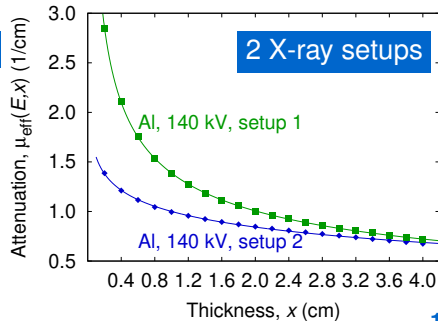
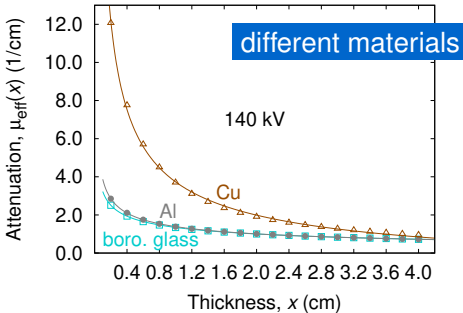
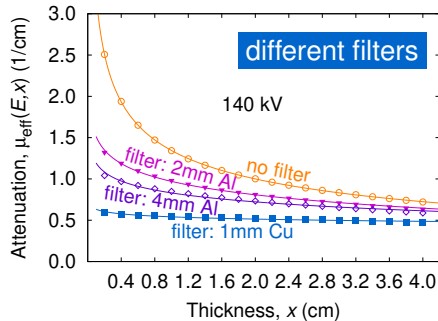
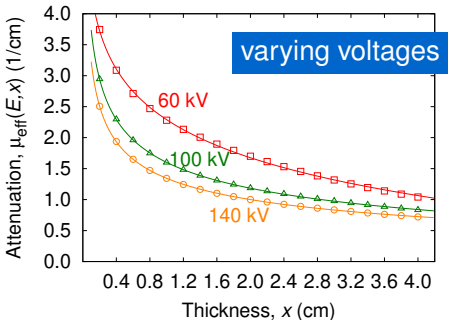
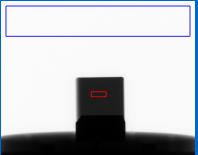
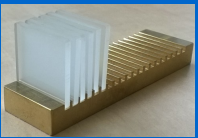
Universality of
 $\mu_{\text{eff}}(x) = a + \frac{b}{x^\alpha}$



Universality of
 $\mu_{\text{eff}}(x) = a + \frac{b}{x^\alpha}$



Universality of
 $\mu_{\text{eff}}(x) = a + \frac{b}{x^\alpha}$



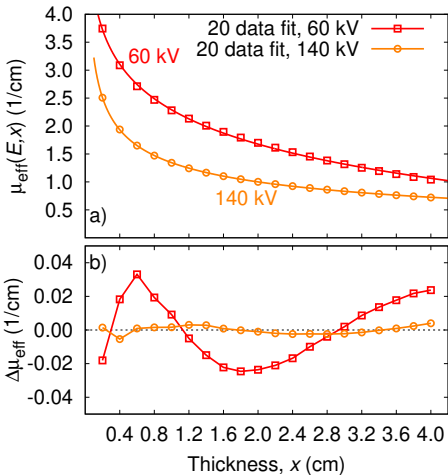
Determining the material thickness x

Generalized Beer-Lambert

$$I(x) = I_0 \exp(-\mu_{\text{eff}}(x) x)$$

Model function

$$\mu_{\text{eff}}(x) = a + \frac{b}{x^\alpha}$$



Determining the material thickness x

Generalized Beer-Lambert

$$I(x) = I_0 \exp(-\mu_{\text{eff}}(x) x)$$

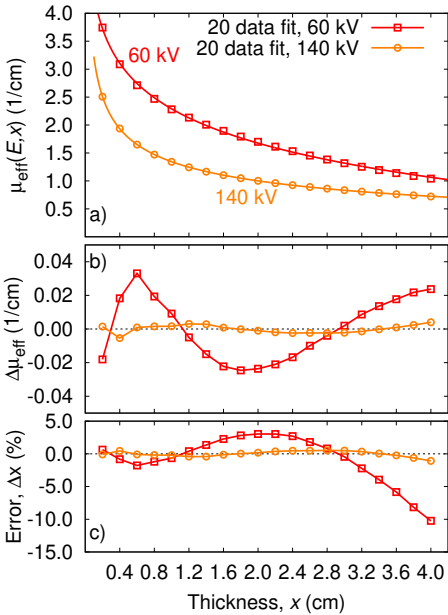
Model function

$$\mu_{\text{eff}}(x) = a + \frac{b}{x^\alpha}$$

Solve

$$ax + bx^{1-\alpha} + \ln\left(\frac{I(x)}{I_0}\right) = 0$$

e.g. Newton's method or look-up table



Determining the material thickness x

Generalized Beer-Lambert

$$I(x) = I_0 \exp(-\mu_{\text{eff}}(x) x)$$

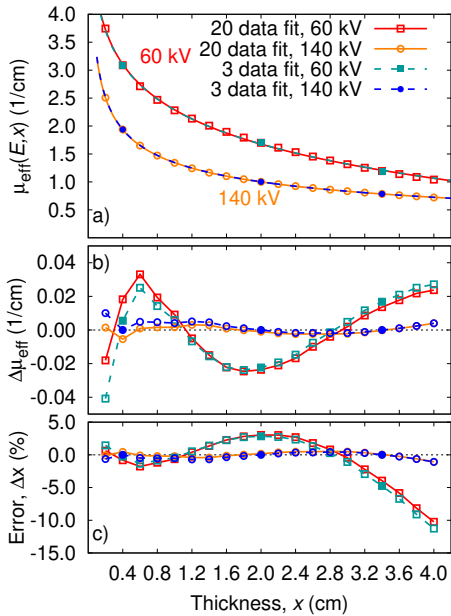
Model function

$$\mu_{\text{eff}}(x) = a + \frac{b}{x^\alpha}$$

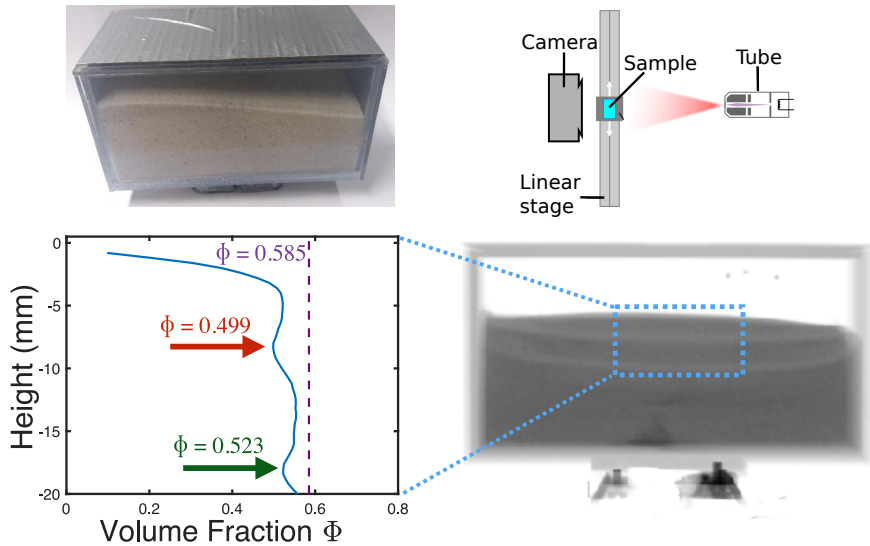
Solve

$$ax + bx^{1-\alpha} + \ln\left(\frac{I(x)}{I_0}\right) = 0$$

e.g. Newton's method or look-up table

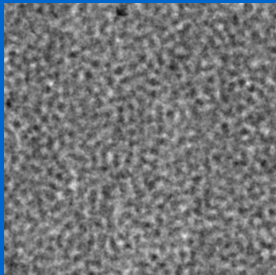


Migrating shear bands in shaken granular matter, Kollmer *et al* (2020)

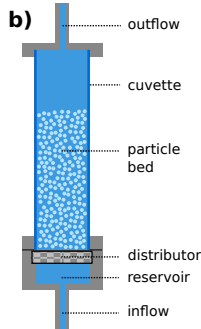
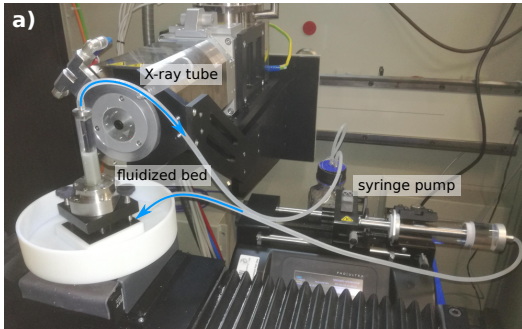


X-ray Digital Fourier Analysis (X-DFA)

A technique to measure granular dynamics

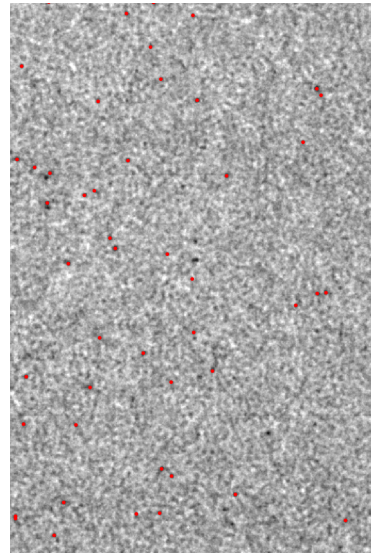
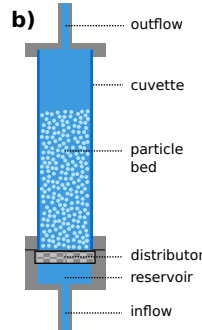
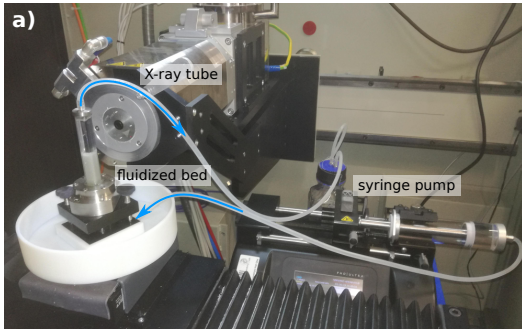


Experiments



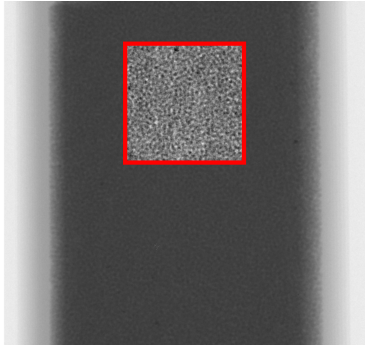
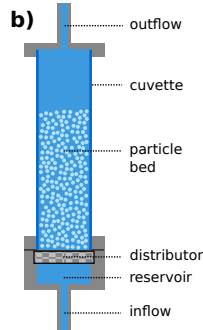
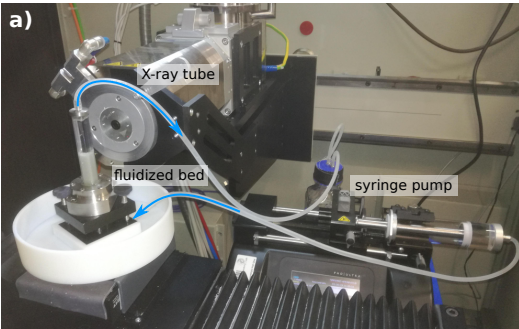
- volume fraction: $0.45 < \Phi < 0.56$
- control dynamics and Φ via pump rate

Experiments

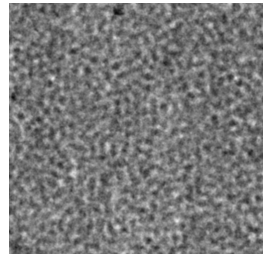


- volume fraction: $0.45 < \Phi < 0.56$
- control dynamics and Φ via pump rate

Experiments



- volume fraction: $0.45 < \Phi < 0.56$
- control dynamics and Φ via pump rate



Differential Dynamic Microscopy (DDM)

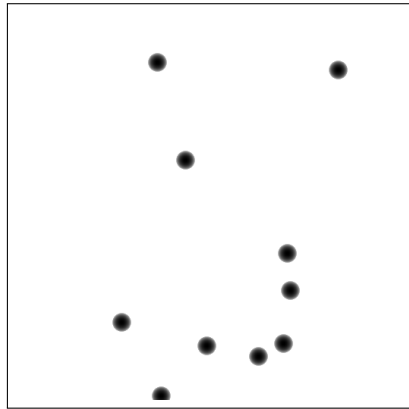
	up to now	this work
system	dispersion, gels	fluidized bed
particles	colloids	granulate
part. diameter	$< 1 \mu\text{m}$	$\approx 200 \mu\text{m}$
volume fraction	$\Phi \leq 0.33$	$0.45 < \Phi < 0.56$
imaging	light microscope	x-ray radiography
dynamics	Brownian motion, caging, glassy, collective motion	

Extending Differential Dynamic Microscopy (DDM) to X-ray imaging

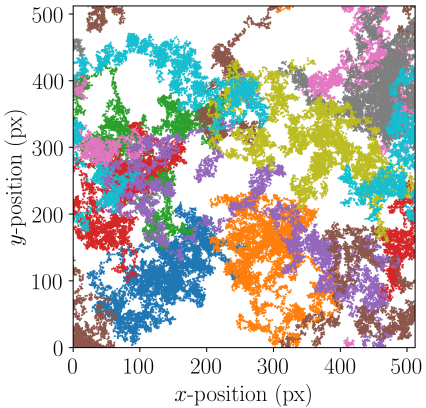
	up to now	this work
system	dispersion, gels	fluidized bed
particles	colloids	granulate
part. diameter	$< 1 \mu\text{m}$	$\approx 200 \mu\text{m}$
volume fraction	$\Phi \leq 0.33$	$0.45 < \Phi < 0.56$
imaging	light microscope	x-ray radiography
dynamics	Brownian motion, caging, glassy, collective motion	

Digital Fourier Analysis of X-Ray Radiograms (X-DFA)

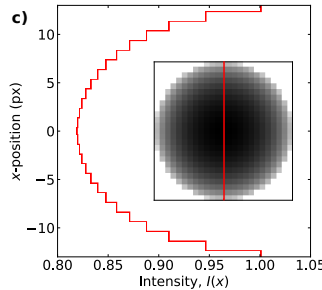
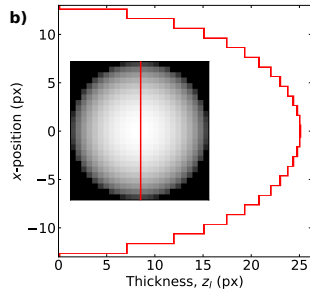
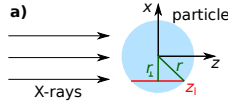
Synthetic radiograms



Video 10 Particles

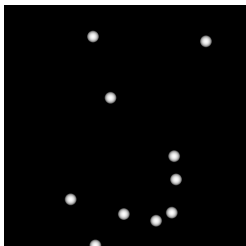
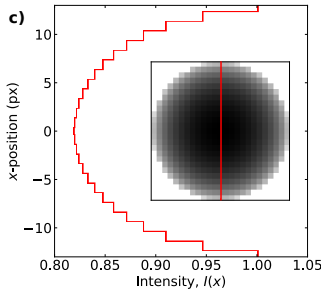
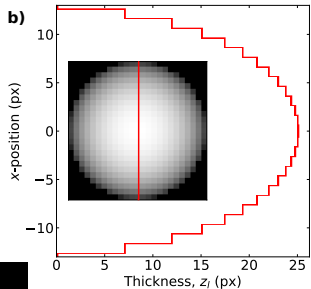
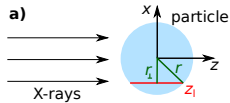


Synthetic radiograms

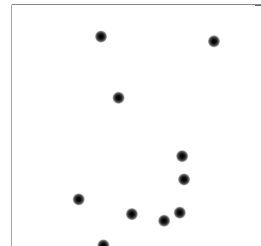


Beer-Lambert
 $I(z_I) = I_0 \exp(-\mu z)$

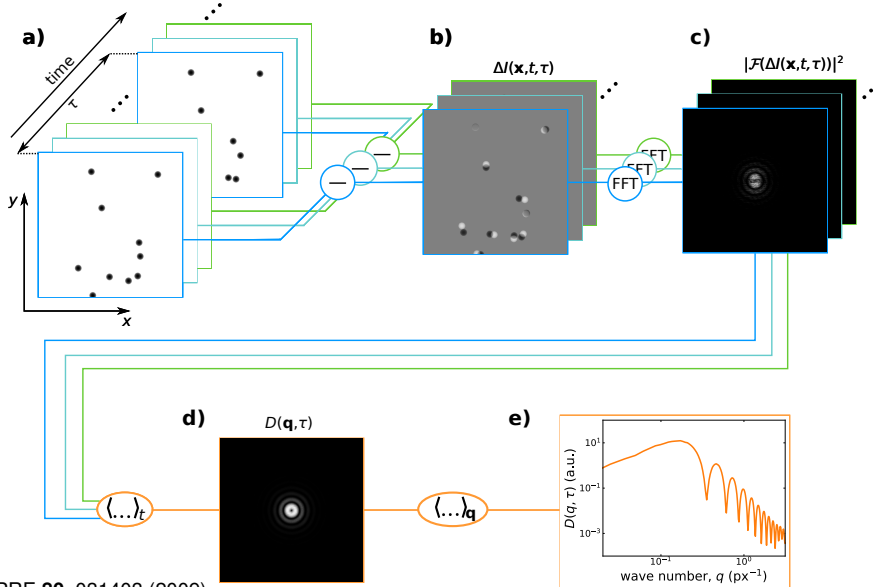
Synthetic radiograms



Beer-Lambert
 $I(z_l) = I_0 \exp(-\mu z)$

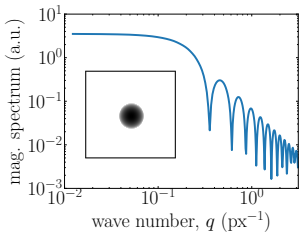
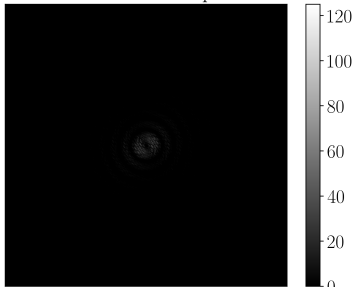


The image structure function $D(\mathbf{q}, \tau)$



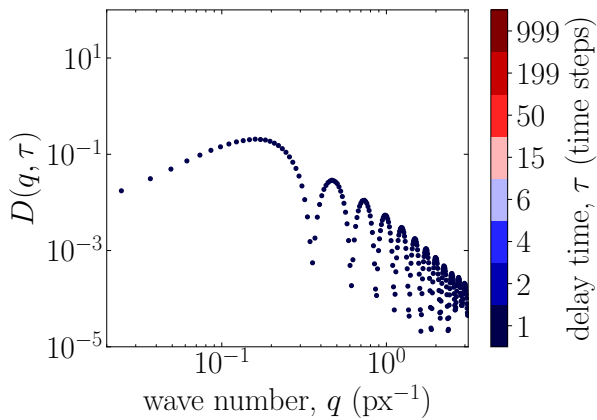
The image structure function $D(q, \tau)$

$\tau = 1$ time steps



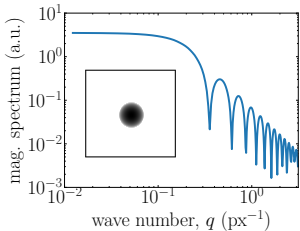
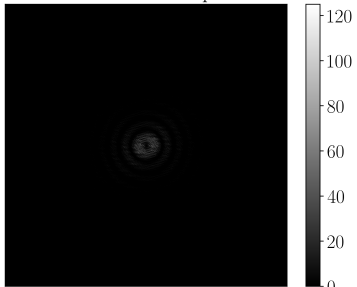
Time averaging: $D(\mathbf{q}, \tau) = \langle |\mathcal{F}(\Delta I)|^2 \rangle_t$

Azimuthal averaging: $D(\mathbf{q}, \tau) \rightarrow D(\mathbf{q}, \tau) \dots$



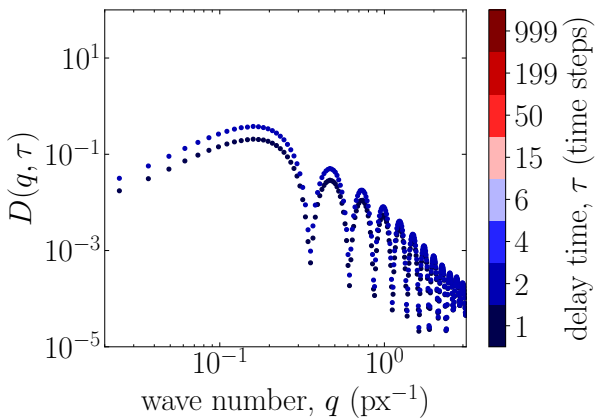
The image structure function $D(q, \tau)$

$\tau = 2$ time steps



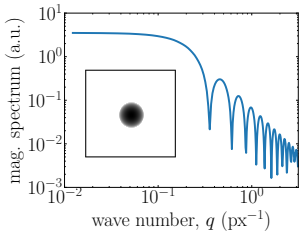
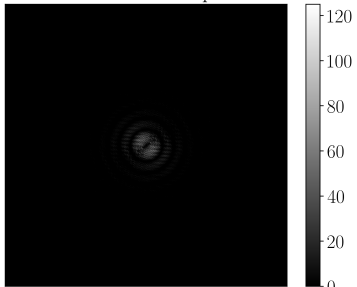
Time averaging: $D(\mathbf{q}, \tau) = \langle |\mathcal{F}(\Delta I)|^2 \rangle_t$

Azimuthal averaging: $D(\mathbf{q}, \tau) \rightarrow D(\mathbf{q}, \tau) \dots$



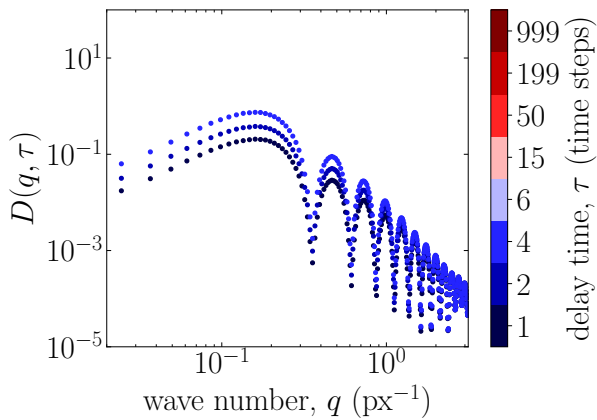
The image structure function $D(q, \tau)$

$\tau = 4$ time steps



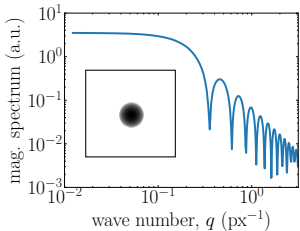
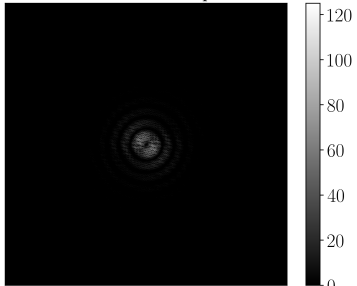
Time averaging: $D(\mathbf{q}, \tau) = \langle |\mathcal{F}(\Delta I)|^2 \rangle_t$

Azimuthal averaging: $D(\mathbf{q}, \tau) \rightarrow D(\mathbf{q}, \tau) \dots$



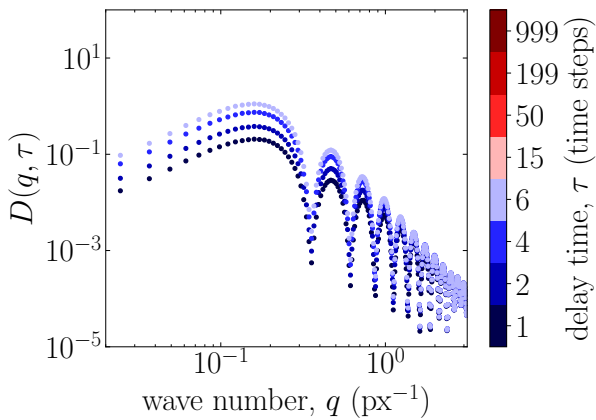
The image structure function $D(q, \tau)$

$\tau = 6$ time steps

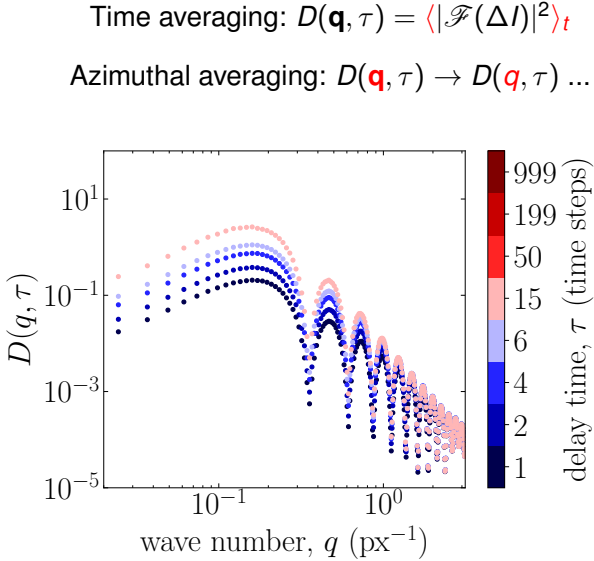
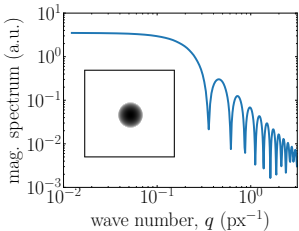
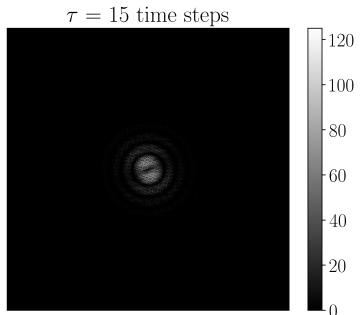


Time averaging: $D(\mathbf{q}, \tau) = \langle |\mathcal{F}(\Delta I)|^2 \rangle_t$

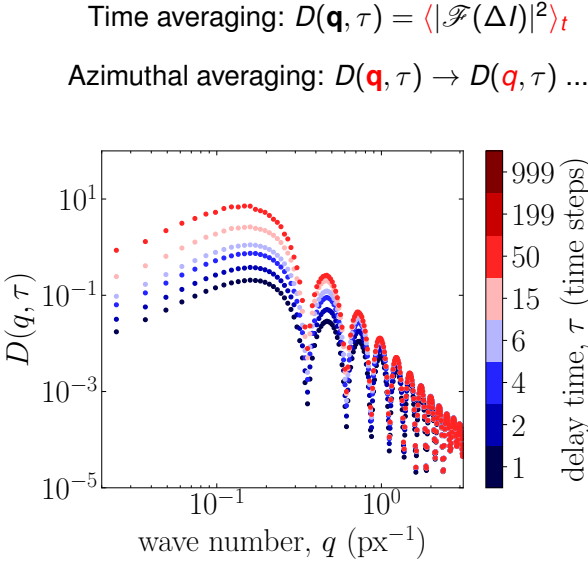
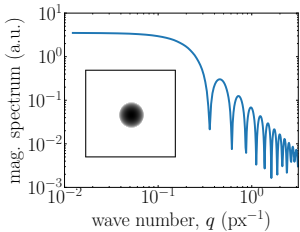
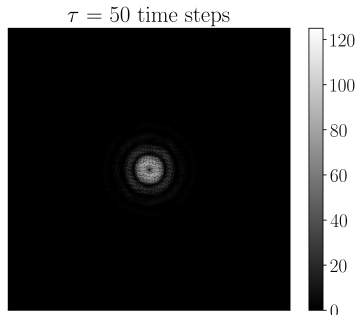
Azimuthal averaging: $D(\mathbf{q}, \tau) \rightarrow D(\mathbf{q}, \tau) \dots$



The image structure function $D(q, \tau)$

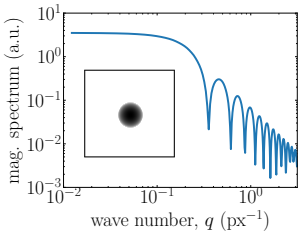
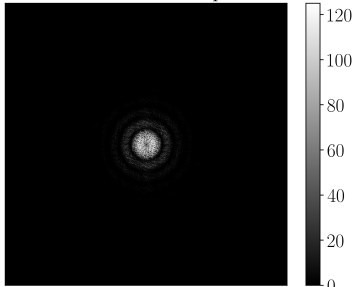


The image structure function $D(q, \tau)$



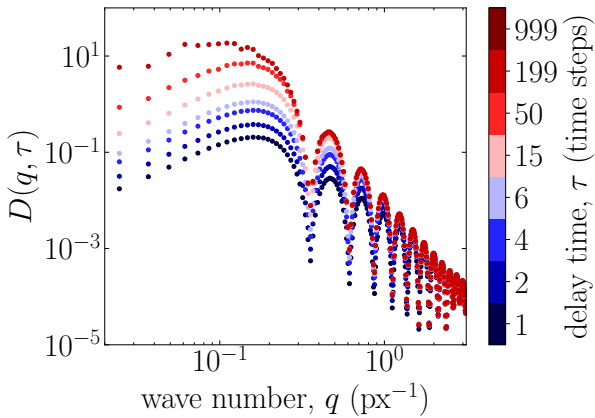
The image structure function $D(q, \tau)$

$\tau = 199$ time steps



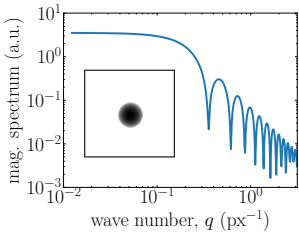
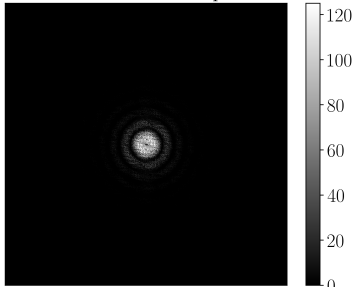
Time averaging: $D(\mathbf{q}, \tau) = \langle |\mathcal{F}(\Delta I)|^2 \rangle_t$

Azimuthal averaging: $D(\mathbf{q}, \tau) \rightarrow D(\mathbf{q}, \tau) \dots$



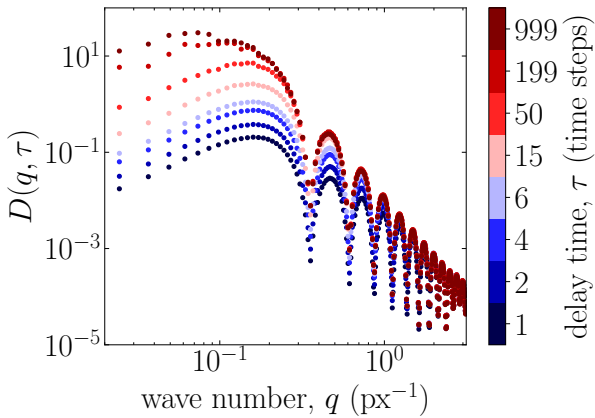
The image structure function $D(q, \tau)$

$\tau = 999$ time steps

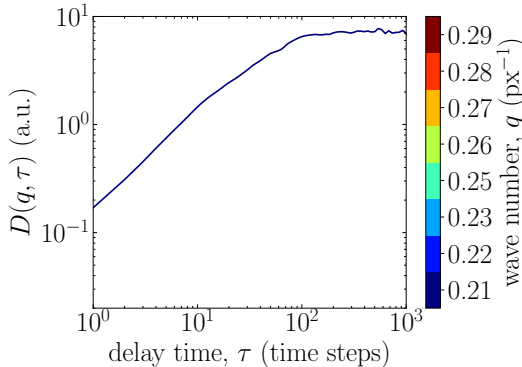
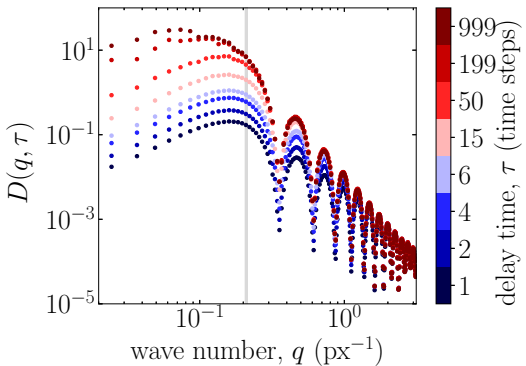


Time averaging: $D(\mathbf{q}, \tau) = \langle |\mathcal{F}(\Delta I)|^2 \rangle_t$

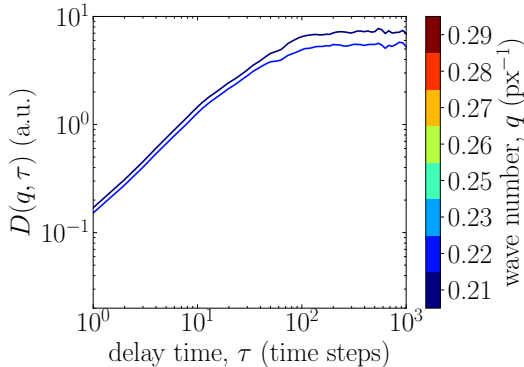
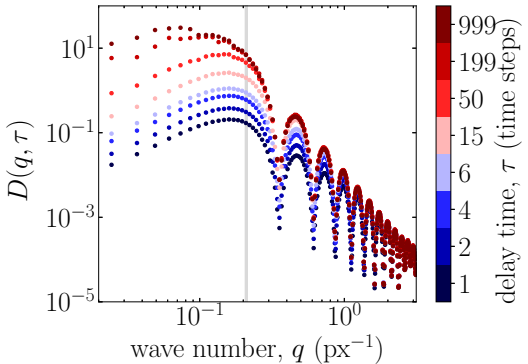
Azimuthal averaging: $D(\mathbf{q}, \tau) \rightarrow D(\mathbf{q}, \tau) \dots$



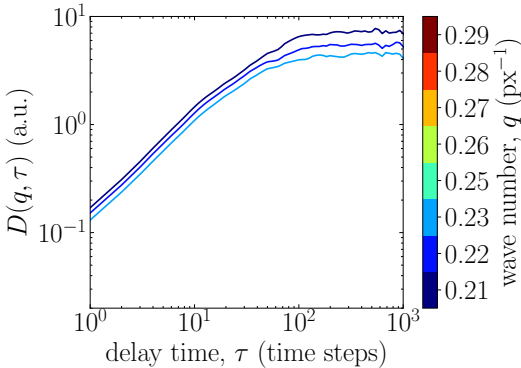
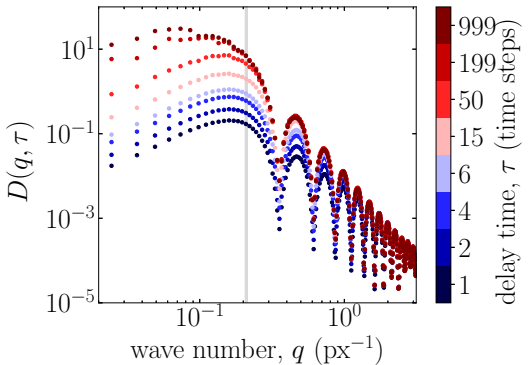
The image structure function $D(q, \tau)$



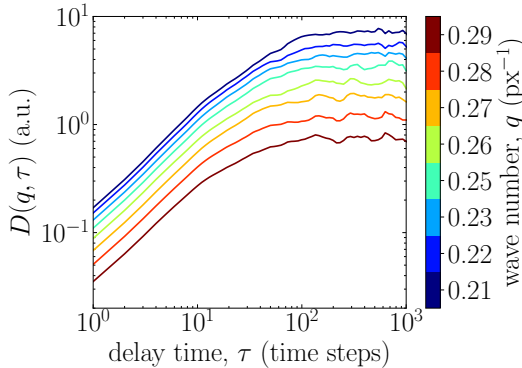
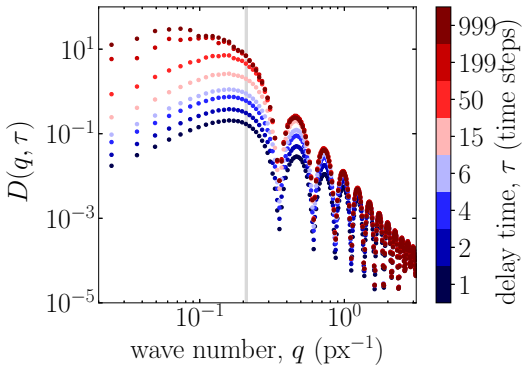
The image structure function $D(q, \tau)$



The image structure function $D(q, \tau)$

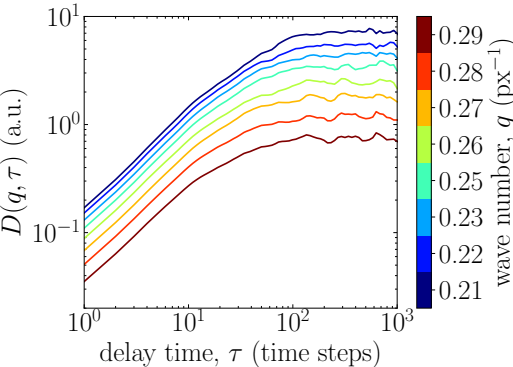
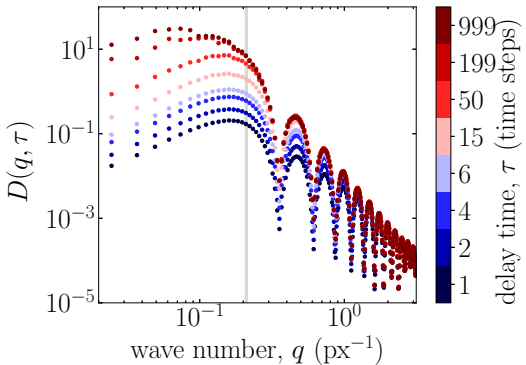


The image structure function $D(q, \tau)$



$$\begin{aligned}
 D(q, \tau) &= \left\langle |I(q, t + \tau) - I(q, t)|^2 \right\rangle_t \\
 &= A(q) \left[1 - \frac{\left\langle I^*(q, t) I(q, t + \tau) \right\rangle_t}{\left\langle |I(q, t)|^2 \right\rangle_t} \right] + B(q)
 \end{aligned}$$

The image structure function $D(q, \tau)$



$$\begin{aligned}
 D(q, \tau) &= \left\langle |I(q, t + \tau) - I(q, t)|^2 \right\rangle_t \\
 &= A(q) \left[1 - \underbrace{\frac{\langle I^*(q, t) I(q, t + \tau) \rangle_t}{\langle |I(q, t)|^2 \rangle_t}}_{\text{image correlation function}} \right] + B(q)
 \end{aligned}$$

Linear space invariant imaging

image correlation function

$$g(\mathbf{q}, \tau) = \frac{\langle I^*(\mathbf{q}, t) I(\mathbf{q}, t + \tau) \rangle_t}{\langle |I(\mathbf{q}, t)|^2 \rangle_t}$$

Linear space invariant imaging

image correlation function

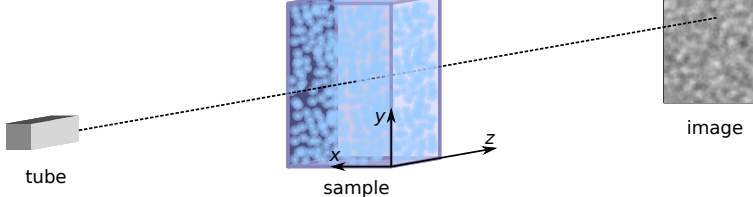
$$g(\mathbf{q}, \tau) = \frac{\langle I^*(\mathbf{q}, t)I(\mathbf{q}, t + \tau) \rangle_t}{\langle |I(\mathbf{q}, t)|^2 \rangle_t}$$

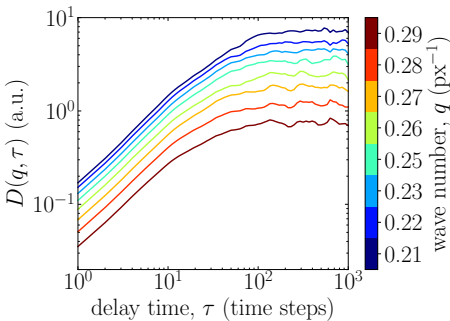
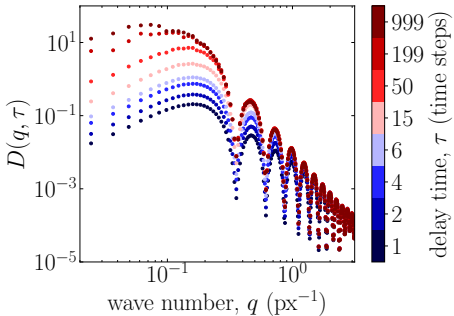
intermediate scattering function

$$f(\mathbf{q}, \tau) = \frac{\langle \rho^*(\mathbf{q}, t)\rho(\mathbf{q}, t + \tau) \rangle_t}{\langle |\rho(\mathbf{q}, t)|^2 \rangle_t}$$

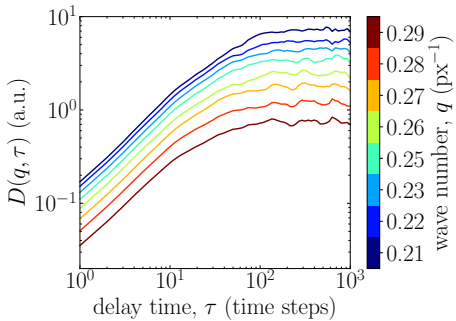
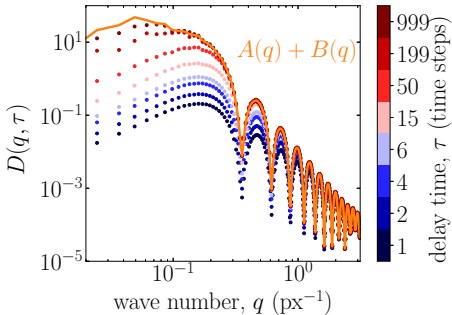
Linear space-invariant imaging:

$$I(\mathbf{r}, t) = I_0 + \int d\mathbf{r}' dz' T(\mathbf{r} - \mathbf{r}', -z') c(\mathbf{r}', z', t)$$



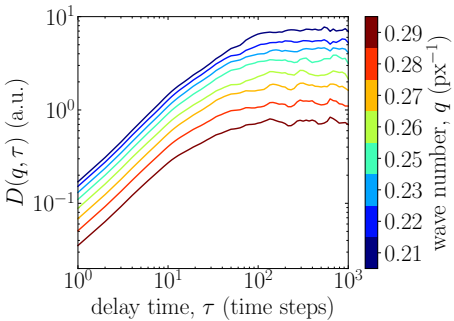
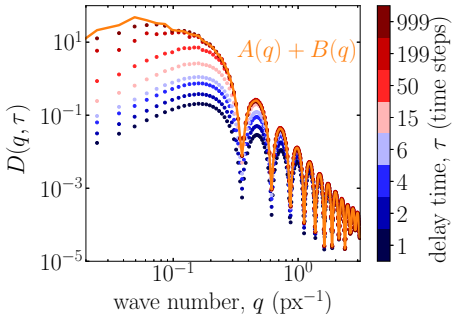


$$\begin{aligned}
 D(q, \tau) &= \left\langle |I(q, t + \tau) - I(q, t)|^2 \right\rangle_t \\
 &= A(q) \underbrace{\left[1 - \frac{\langle I^*(q, t) I(q, t + \tau) \rangle_t}{\langle |I(q, t)|^2 \rangle_t} \right]}_{\text{image correlation function}} + B(q)
 \end{aligned}$$



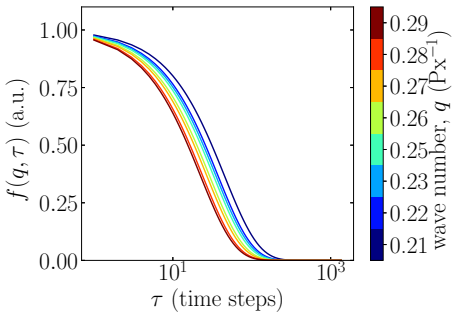
$$\begin{aligned} D(q, \tau) &= \left\langle |I(q, t + \tau) - I(q, t)|^2 \right\rangle_t \\ &= A(q) \left[1 - \frac{\langle I^*(q, t) I(q, t + \tau) \rangle_t}{\langle |I(q, t)|^2 \rangle_t} \right] + B(q) \end{aligned}$$

- $d(q, \tau \rightarrow 0) = B(q) = 0$
- $d(q, \tau \rightarrow 0) = A(q) + B(q)$

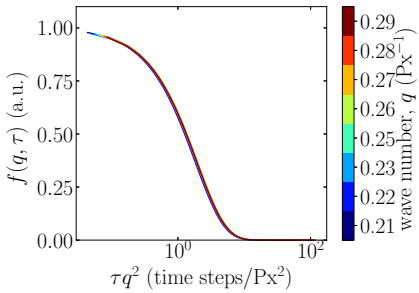
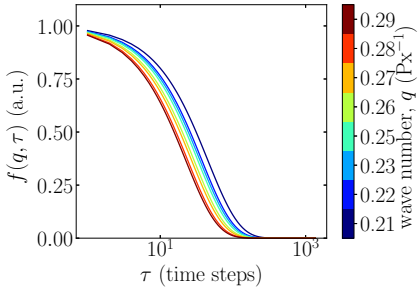


$$\begin{aligned} D(q, \tau) &= \left\langle |I(q, t + \tau) - I(q, t)|^2 \right\rangle_t \\ &= A(q) \left[1 - \frac{\langle I^*(q, t) I(q, t + \tau) \rangle_t}{\langle |I(q, t)|^2 \rangle_t} \right] + B(q) \end{aligned}$$

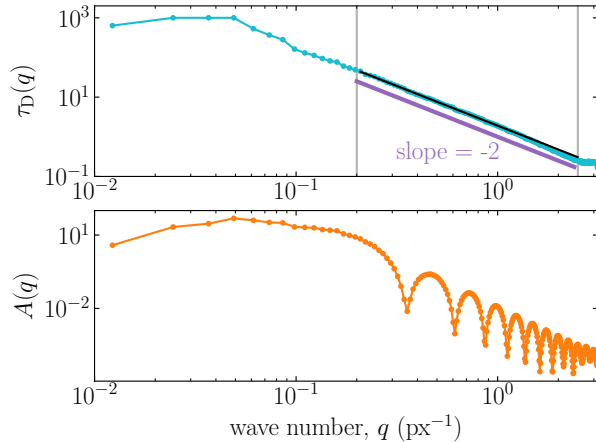
- $d(q, \tau \rightarrow 0) = B(q) = 0$
- $d(q, \tau \rightarrow 0) = A(q) + B(q)$



Intermediate scattering function $f(q, \tau)$



Brownian motion:
 $f(q, \tau) = \exp(-q^2\tau/\tau_D)$
Accuracy: 2% - 6%

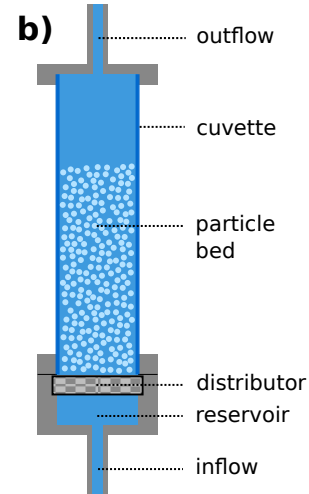
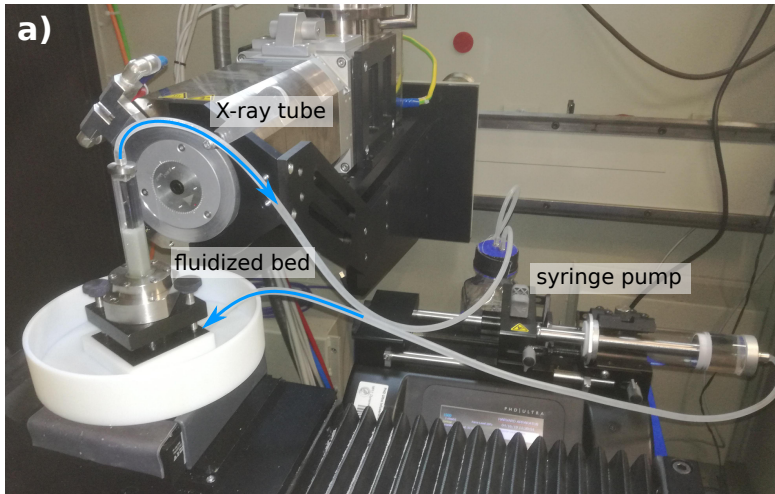


Validating X-DFA on a sedimenting
suspension

Measurements on a fluidized bed

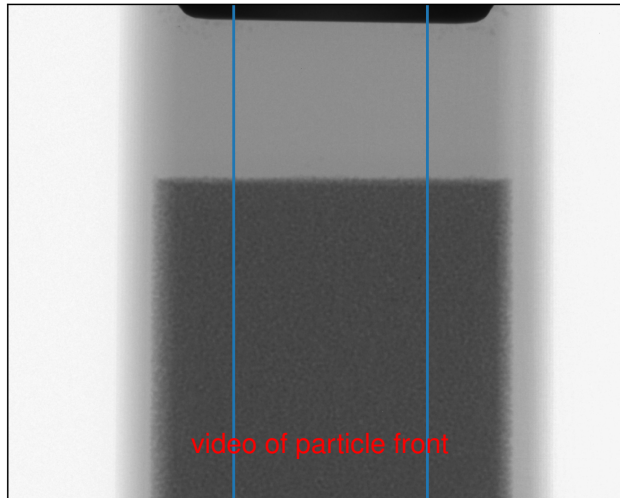
Experimental validation: Sedimenting suspension

track sedimentation front ↔ DFA

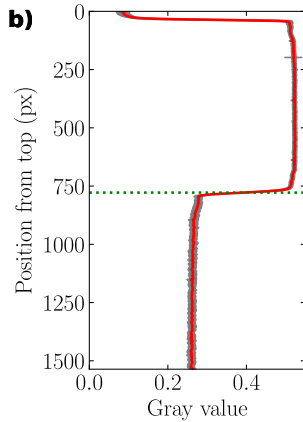
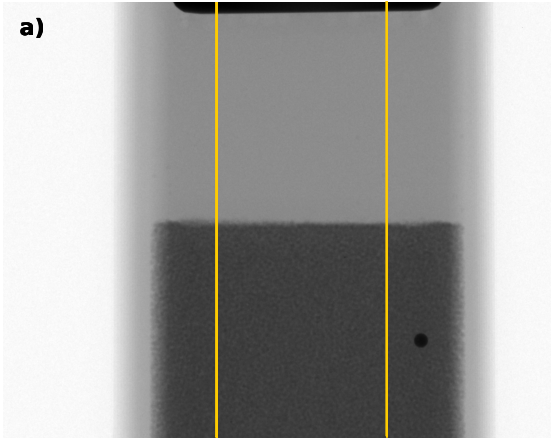


Experimental validation: Sedimenting suspension

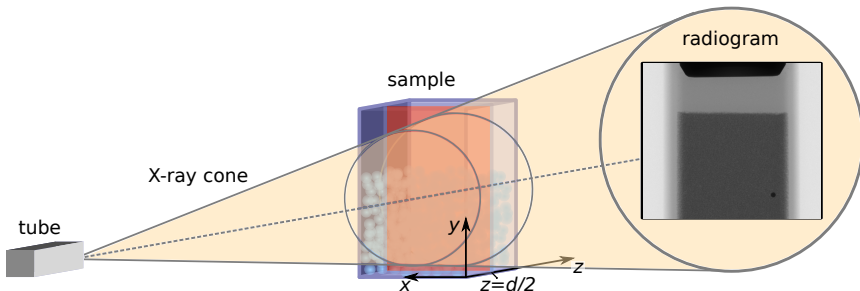
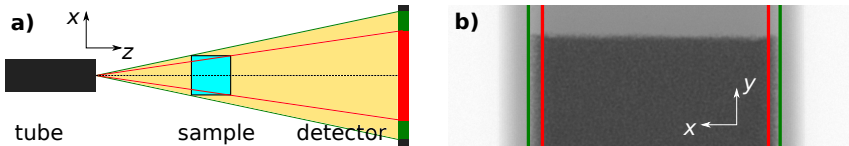
track sedimentation front ↔ DFA



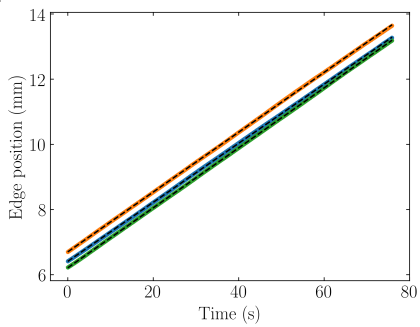
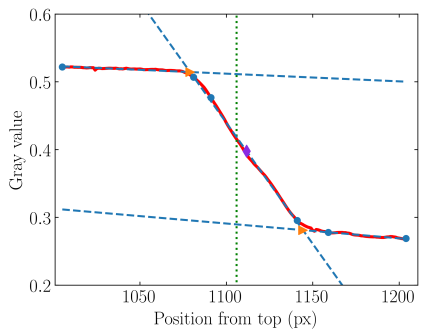
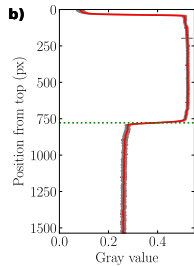
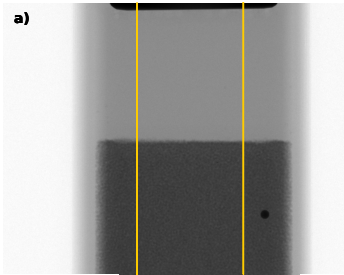
Tracking of particle front



Tracking of particle front

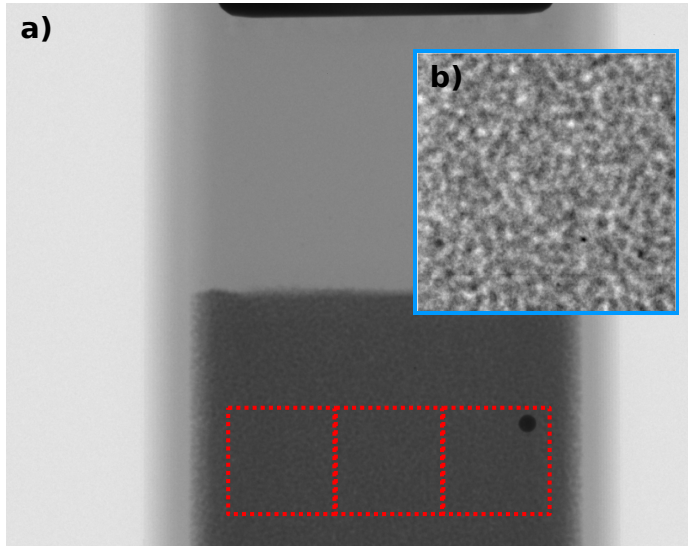


Tracking of particle front

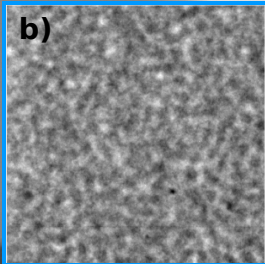


X-DFA for sedimenting particles

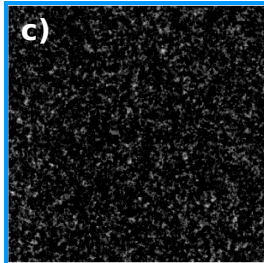
a)



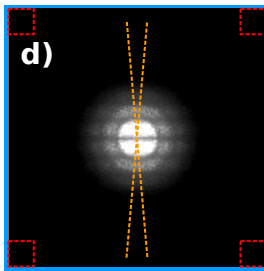
b)



c)

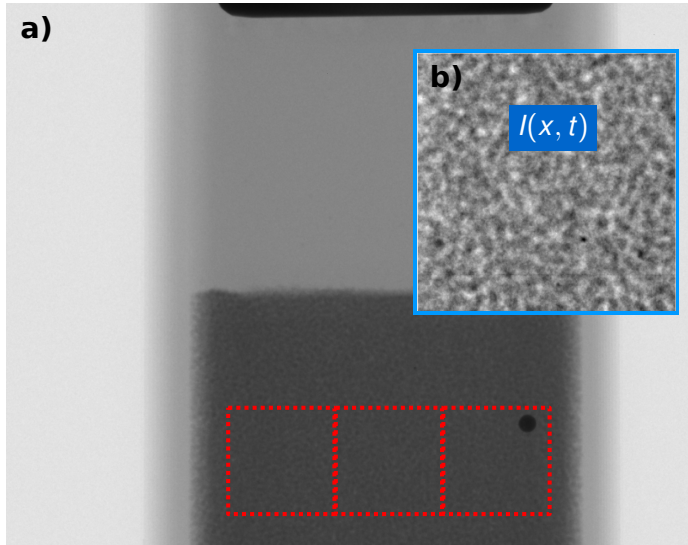


d)



X-DFA for sedimenting particles

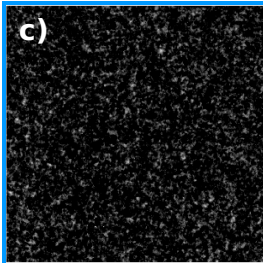
a)



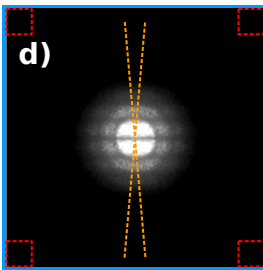
b)

$$I(x, t)$$

c)

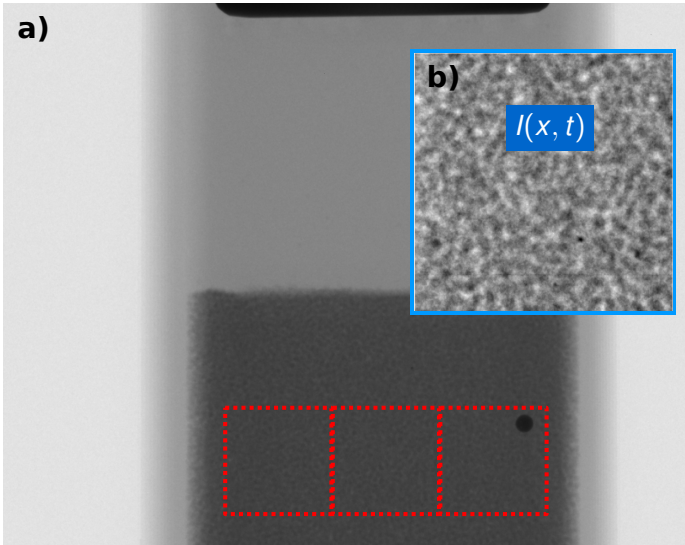


d)

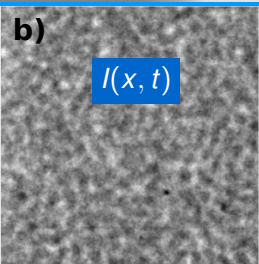


X-DFA for sedimenting particles

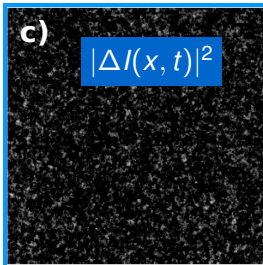
a)



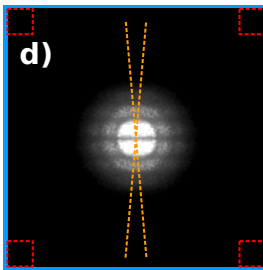
b)



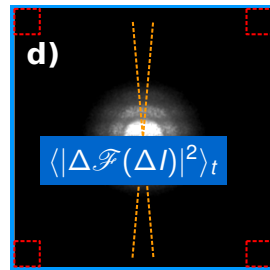
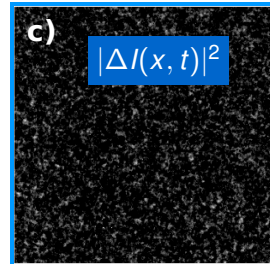
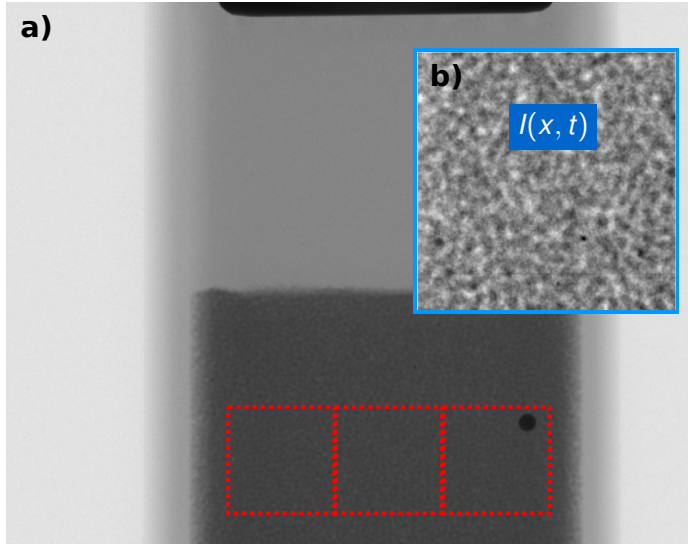
c)



d)



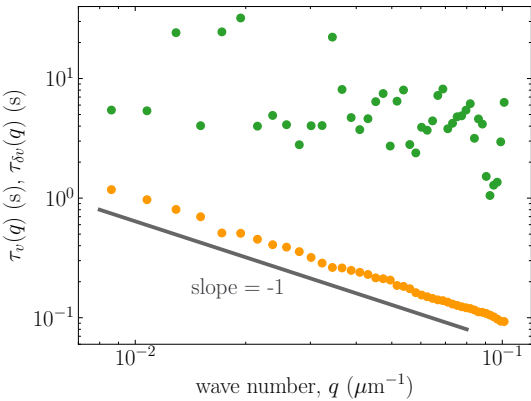
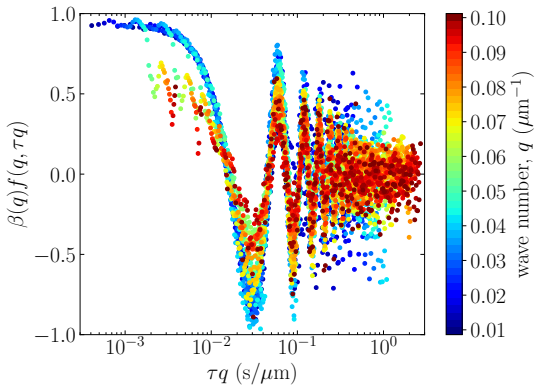
X-DFA for sedimenting particles



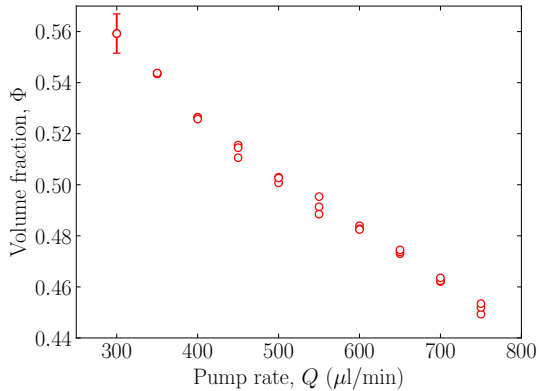
X-DFA for sedimenting particles

$$f(q, \tau) = \cos(q\langle v_s \rangle \tau) \exp\left(-\frac{1}{2}q^2 \delta v^2 \tau^2\right)$$

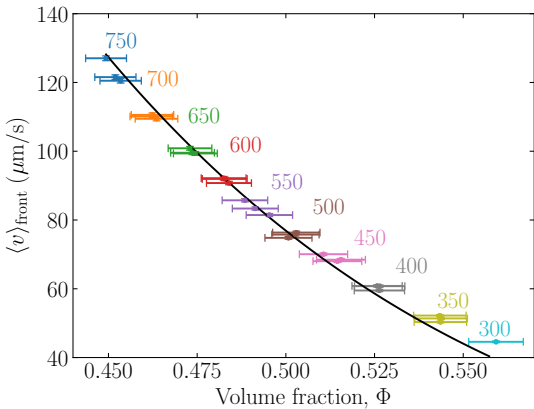
$$\langle v_s \rangle = \langle \Delta r \rangle / \tau_\nu, \langle \delta v \rangle = \langle \delta r \rangle / \tau_{\delta\nu}$$



Richardson-Zaki law

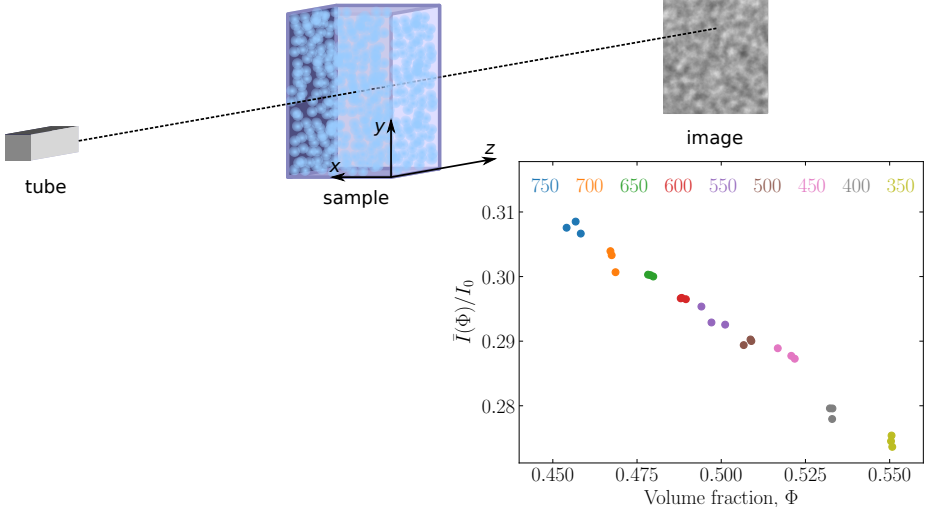


$$\frac{\langle v \rangle_{\text{front}}}{v_{\text{Stokes}}} = (1 - \Phi)^n$$

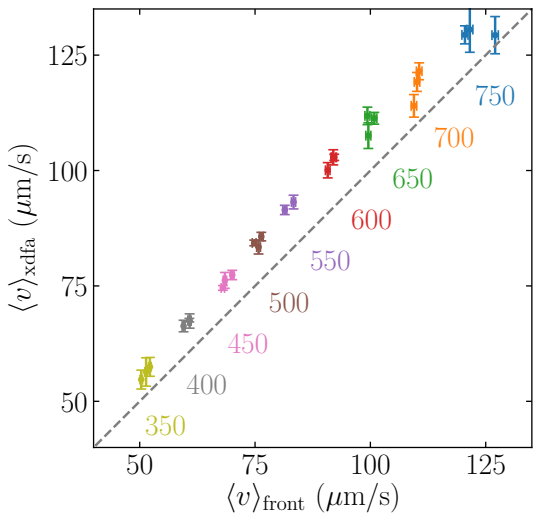


X-DFA: Requirement of linear space invariant imaging

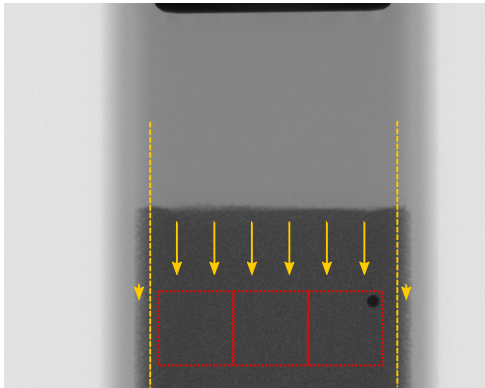
$$I(\mathbf{r}, t) = I_0 + \int d\mathbf{r}' dz' T(\mathbf{r} - \mathbf{r}', -z') c(\mathbf{r}', z', t)$$



Front tracking vs. X-DFA

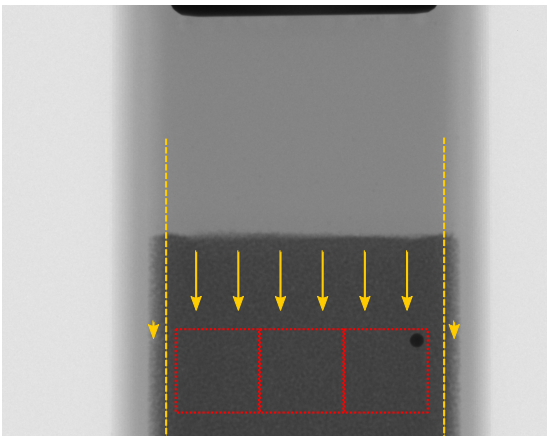


$\langle v \rangle_{\text{xdfa}} > \langle v \rangle_{\text{front}}$ by 9.4%



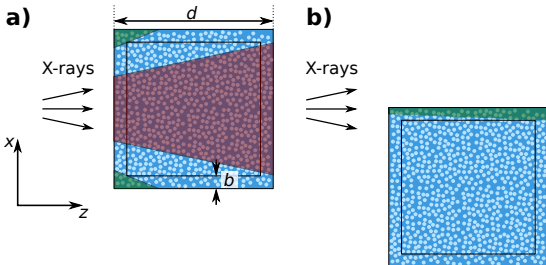
sample video

Estimate width of boundary layer



$\langle v \rangle_{\text{xdfa}} > \langle v \rangle_{\text{front}}$ by 9.4%

$\langle v \rangle_{\text{xdfa}}$ takes two layers into account
 $\langle v \rangle_{\text{front}}$ takes four layers into account



Estimation:

Boundary velocity = 0

Else = const.

→ $b \approx 3$ particle diameters

Thank you for your attention!

